2026 IEEE International Conference on Robotics and Automation (ICRA 2026)
June 1-5, 2026. Vienna, Austria

# Symmetry-Aware Skill Transfer with Energy-Tank Passive Control for Ankle Exoskeletons

1st Etienne Largeteau
*IBISC Laboratory*
*University of Paris-Saclay*
Paris, France
etienne.largeteau@ens-paris-saclay.fr

2nd Lokman Bencharif
*IBISC Laboratory*
*University of Paris-Saclay*
Paris, France

3rd Bangaly Conté
*IBISC Laboratory*
*University of Paris-Saclay*
Paris, France

4th Abderahim Ibset
*IBISC Laboratory*
*University of Paris-Saclay*
Paris, France

5th Hang Su
*IBISC Laboratory*
*University of Paris-Saclay*
Paris, France
hang.su@univ-evry.fr

6th Olivier Bruneau
*LURPA*
*ENS Paris-Saclay, Université Paris-Saclay*
Paris, France
olivier.bruneau@ens-paris-saclay.fr

7th Samer Alfayad
*IBISC Laboratory*
*University of Paris-Saclay*
Paris, France
samer.alfayad@univ-evry.fr

***Abstract*—This paper presents a unified framework that combines symmetry-aware skill transfer with energy-tank passive control to achieve safe and adaptive ankle exoskeleton assistance. Subject-specific ankle references are first extracted from wearable IMU data : Dynamic Time Warping (DTW) aligns gait cycles onto a normalized phase axis , and Gaussian Mixture Regression (GMR) synthesizes smooth probabilistic templates suitable for online modulation. When only unilateral sensing is available, contralateral trajectories are reconstructed through either a half-period phase shift or a DTW-informed nonlinear mapping, enabling robust bilateral assistance. These references are then tracked by a joint-space PID controller wrapped with an energy tank, which bounds power exchange and prevents unintended energy injection. In simulation experiments, the proposed controller improved center-of-mass smoothness relative to plain PID. Benchtop validation confirms the efficacy of both GMR-generated and symmetric-generated trajectories. Furthermore, experimental results show a reduction of 40 N in peak interaction force (from 120 N to 80 N), resulting in less mechanical strain on the user. By unifying phase-consistent gait synthesis with passivity shaping, this work advances ankle exoskeleton assistance that is individualized, robust, and inherently safe.**

***Index Terms*—Rehabilitation robotics; ankle exoskeletons; gait analysis; symmetry-aware skill transfer; passivity-based control; wearable sensing**

## I. Introduction

Stroke remains a leading cause of long-term disability worldwide [1], and many survivors exhibit persistent gait impairments that reduce independence and quality of life [2]. Such impairments are often characterized by reduced push-off power, altered ankle kinematics, and asymmetry between limbs. These deficits not only compromise mobility but also increase the risk of falls and raise metabolic cost during locomotion, further limiting participation in daily activities. Robotic ankle exoskeletons have emerged as promising tools for rehabilitation and assistance, with the potential to deliver repeatable, programmable, and adaptive support that augments the patient's residual motor function. However, two longstanding hurdles continue to limit their robustness and safety: (i) constructing *subject-specific, phase-consistent* references that remain stable across cadence and timing variability, and (ii) enforcing *interaction safety* so that assistance cannot inject unbounded energy into the human–robot system.

On the reference-learning side, prior work has shown that generic templates or simple temporal rescaling often fail to capture the variability of gait events, particularly during phases such as push-off where timing differs significantly across steps. Dynamic Time Warping (DTW) provides a way to align repeated cycles by compensating for local accelerations and delays, thereby producing phase-normalized data robust to cadence changes [5], [6]. Once aligned, movement-learning approaches such as Gaussian Mixture Regression (GMR) can consolidate multiple trials into a compact probabilistic template that both smooths noise and preserves variability structure [7]. This property is critical for rehabilitation scenarios, where controllers must adapt assistance levels as patients recover or as gait patterns evolve. Moreover, clinical practice often involves unilateral sensing (e.g., measuring only the less-affected limb), making contralateral synthesis a necessity.

Symmetry-based reconstruction—whether via half-period phase shifts or nonlinear mappings informed by DTW—offers a principled way to extend unilateral sensing into bilateral assistance, directly addressing a central clinical goal: restoring gait symmetry.

On the control side, safety remains non-negotiable in human–robot interaction. While high-gain controllers can achieve accurate trajectory tracking, they risk injecting unbounded energy into the coupled system, potentially destabilizing the user or inducing discomfort.

979-8-3315-8160-2/26/$31.00 ©2026 IEEE

Control paradigms for ankle exoskeletons span myoelectric (EMG-driven) and event-based timing control to neuromuscular model-based adaptive schemes, illustrating the diversity of user–device interfaces and assistance timing [19], [20]. Passivity-based control has become a standard approach to mitigate this risk by guaranteeing that the closed-loop system cannot generate net energy. Among various implementations, energy-tank architectures are particularly attractive because they introduce a virtual reservoir that monitors stored energy and gates torque commands accordingly [9]–[11]. When the tank depletes, the controller automatically becomes more conservative, ensuring passivity at the expense of some tracking precision. This trade-off is well aligned with rehabilitation requirements, where safety and user comfort outweigh perfect trajectory tracking.

Building on these challenges, we propose a unified framework that couples subject-specific gait reference learning with passivity-guaranteed control. DTW aligns repeated gait cycles onto a normalized phase axis, and GMR consolidates them into smooth probabilistic templates. With unilateral sensing, contralateral trajectories are reconstructed via half-period symmetry or DTW-informed nonlinear mapping, enabling robust unilateral-to-bilateral skill transfer. On the control side, a joint-space PID is wrapped by an energy-tank layer that adaptively gates effort according to stored virtual energy, preventing unsafe power injection into the human–robot system.

The main contributions of this paper are summarized as follows:

1) A symmetry-aware skill transfer pipeline that learns subject-specific ankle templates from wearable IMU data using DTW–GMR and reconstructs contralateral references from unilateral sensing.
2) An energy-tank–based passive control scheme that bounds power exchange through adaptive torque gating, guaranteeing safety even under timing errors or aggressive setpoints.
3) A comprehensive evaluation in simulation and benchtop experiments, showing a 40 N reduction in peak interaction force and improved CoM smoothness compared with plain PID.

## II. Phase-Consistent Gait Reference Learning via DTW and GMR

The goal of this section is to construct subject-specific reference ankle trajectories that are consistent across steps and amenable to safe exoskeleton control. Raw IMU recordings are first converted into ankle joint angles, then temporally aligned with Dynamic Time Warping (DTW), and finally synthesized into smooth probabilistic templates using Gaussian Mixture Regression (GMR). For completeness, we also retain polynomial interpolation as a baseline for comparison.

### A. Data Acquisition and Ankle Angle Estimation

To construct individualized references, kinematics were recorded with two IMUs affixed to the shank and foot, as shown in Fig. 1. Each sensor provided orientation quaternions $q_{\text{shank}}(t)$ and $q_{\text{foot}}(t)$ in the Earth frame. The relative orientation

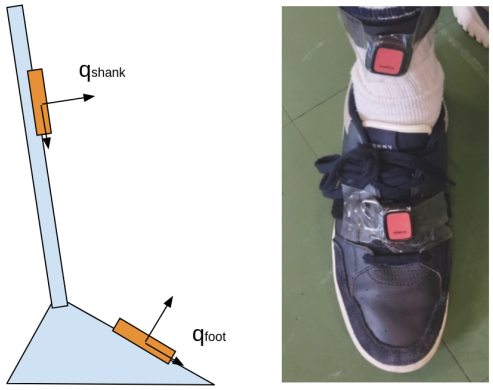


Fig. 1: Placement of IMUs on the shank and foot for ankle angle measurement.

$$q_{\text{rel}}(t) = q_{\text{shank}}^{-1}(t)\, q_{\text{foot}}(t) \tag{1}$$

was projected onto the anatomical flexion axis to yield the ankle angle $\theta_a(t)$ following standard IMU-based procedures [13].

Data were collected from two healthy participants walking along a straight path. For each subject, five repetitions per limb were recorded, yielding sufficient cycles for constructing mean trajectories. Both left and right ankle angles were available, enabling later evaluation of contralateral reconstruction.

### B. Dynamic Time Warping for Trajectory Alignment

Direct averaging of raw trajectories is problematic because gait cycles vary in duration and timing, which blurs critical events such as heel-strike and toe-off. DTW addresses this by nonlinearly re-indexing each cycle onto a normalized phase axis $\phi \in [0, 1]$, ensuring that salient events are aligned across repetitions.

Formally, given two sequences

$$x = (x_1, \ldots, x_N), \quad r = (r_1, \ldots, r_M),$$

DTW seeks an alignment path $W = \{(i_\ell, j_\ell)\}_{\ell=1}^{L}$ that minimizes

$$DTW(x, r) = \min_{W} \sum_{\ell=1}^{L} (x_{i_\ell} - r_{j_\ell})^2, \tag{2}$$

subject to continuity and monotonicity constraints. The recursion

$$D_{i,j} = (x_i - r_j)^2 + \min(D_{i-1,j}, D_{i,j-1}, D_{i-1,j-1}) \tag{3}$$

yields the optimal cost, and backtracking retrieves the alignment path $W^\star$.

**Application to ankle trajectories.** For each subject, all ankle cycles were phase-normalized with DTW, as illustrated in Fig. 2. The top panel shows raw trajectories where inter-cycle variability obscures gait events, while the bottom panel

shows DTW-aligned signals with events consistently synchronized. This alignment provides a common phase domain where smooth reference trajectories can be constructed. We then apply GMR to generate probabilistic templates.

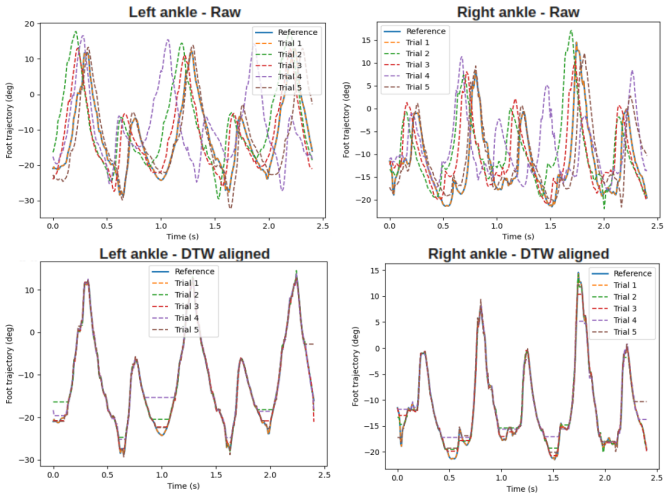


Fig. 2: Effect of DTW alignment. Top: raw ankle trajectories with large timing variability across repetitions. Bottom: DTW-aligned trajectories, showing consistent phase synchronization and improved overlap between steps.

### C. Trajectory Synthesis via GMR

After phase-normalization with DTW, the next step is to synthesize a smooth reference trajectory that captures both the central tendency and variability of ankle motion. To this end, we adopt a probabilistic framework based on Gaussian Mixture Regression (GMR).

**Advantages in our context.** Compared to simple averaging, GMR offers two advantages that are particularly relevant for gait rehabilitation: 1) it consolidates multiple noisy cycles into a smooth template while preserving the variance structure, thus avoiding oversmoothing at key gait events such as push-off; 2) it provides a principled mechanism to adapt the reference to new conditions by modulating the Gaussian parameters, enabling subject-specific scaling of cadence or amplitude.

As shown in Fig. 3, from the measured trajectories, a GMR-generated trajectory can be generated. The probabilistic model clearly smooths local noise while retaining event timing, producing a compact reference suitable for both offline analysis and online control.

### D. Symmetry-Based Contralateral Synthesis

In many clinical or wearable settings, only one limb can be instrumented, making contralateral reconstruction necessary. We consider two complementary strategies:

**(i) Ideal symmetry.** A baseline assumption is that gait alternates perfectly between left and right legs. Under this model, the contralateral reference is obtained by a strict half-period phase shift:

$$\theta_{\text{ref}}^{\text{ideal}}(t) = \theta_{\text{ref}}^{\text{base}}(t + 0.5P), \tag{4}$$

where $P$ is the gait period. This approach is computationally simple and physiologically plausible for healthy, symmetric walking.

**(ii) Nonlinear symmetry.** Human gait, however, often deviates from perfect alternation due to pathology, fatigue, or individual asymmetries. To capture these effects, we introduce a nonlinear mapping learned through DTW-based alignment. Let $\theta_L(\phi)$ and $\theta_R(\phi)$ denote the normalized left and right trajectories. We estimate a phase-warping function $f(\phi)$ by minimizing the DTW distance between contralateral trials, yielding:

$$\theta_{\text{ref}}^{\text{nonlinear}}(\phi) = \theta_{\text{ref}}^{\text{base}}(f(\phi)). \tag{5}$$

This mapping enforces a consistent bilateral structure while accounting for subject-specific asymmetries. Consistent with this view, DTW-based symmetry analyses have been shown to sensitively quantify bilateral differences across the full gait cycle, supporting phase-warped contralateral reconstructions [18].

**Discussion.**

The results show that both symmetry models can generate viable contralateral trajectories from unilateral sensing. The ideal half-period shift provides a robust and computationally efficient baseline when gait symmetry can be assumed, whereas the nonlinear DTW-based mapping adapts the phase relationship to better capture subject-specific timing differences. While their RMSE values are broadly comparable, the nonlinear approach may offer advantages in cases of asymmetric or irregular gait, such as in rehabilitation contexts. Together with the DTW–GMR pipeline for phase-consistent trajectory generation, these strategies support the broader goal of enabling *unilateral sensing to bilateral assistance* for practical wearable exoskeleton deployment.

## III. Passivity Control of a Biped Model

To evaluate the proposed trajectory generation framework in a dynamic locomotion context, we integrate it within a simplified biped model actuated at the ankles. Since safe human–robot interaction is a fundamental requirement for rehabilitation devices, particular attention is given to enforcing *passivity* in the closed-loop control. We therefore model each leg as a planar double pendulum coupled through the pelvis, and implement an *energy-tank passivity layer* wrapped around a conventional joint-space PID controller. This section first introduces the mechanical model, then details the passivity-based control scheme, and finally reports simulation evidence highlighting its influence on tracking accuracy and interaction safety.

### A. Model Description

Each leg is represented as a planar shank–foot double pendulum with the pelvis modeled as a rigid body that couples the two limbs; see Fig. 4. The compact dynamics can be written as:

$$M(q)\ddot{q}+C(q,\dot{q})\dot{q}+G(q) = Q_\tau+Q_{\text{contact}}+Q_{\text{limit}}+Q_{\text{hip}}, \tag{6}$$

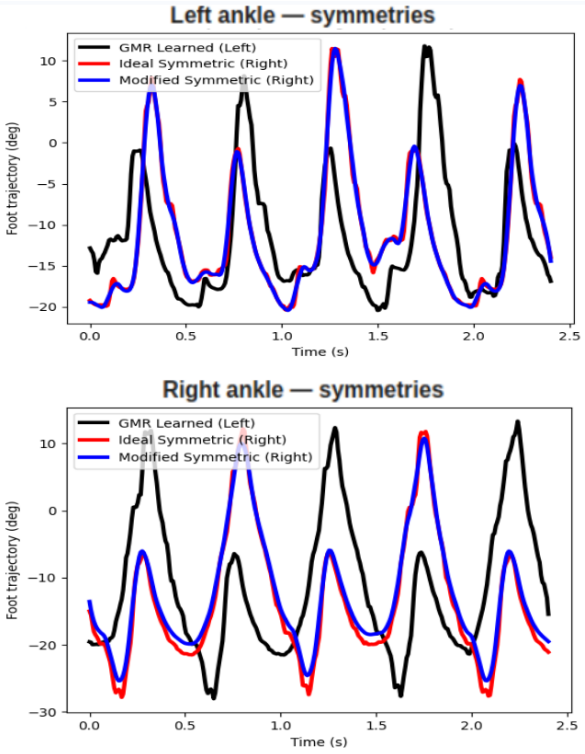


Fig. 3: Comparison of contralateral trajectory generation. Ideal symmetry (dashed) assumes a perfect half-period alternation, whereas nonlinear symmetry (dash-dotted) adapts the phase relationship using DTW-based mapping.

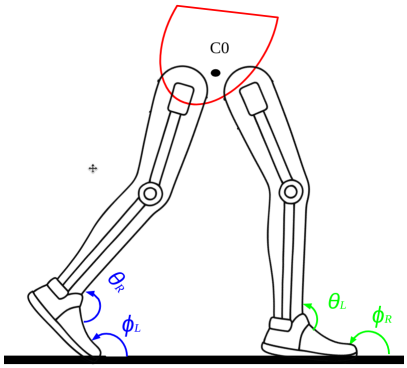


Fig. 4: Planar double-pendulum model. Coordinates: ankle angles $\theta_L, \theta_R$ and foot orientations $\phi_L, \phi_R$.

where $q$ denotes the configuration, $\dot{q}$ the angular velocities, and $\ddot{q}$ the angular accelerations of the system.

$$q = \begin{bmatrix} \phi_L \\ \theta_L \\ \phi_R \\ \theta_R \end{bmatrix}, \quad \dot{q} = \begin{bmatrix} \dot{\phi}_L \\ \dot{\theta}_L \\ \dot{\phi}_R \\ \dot{\theta}_R \end{bmatrix}, \quad \ddot{q} = \begin{bmatrix} \ddot{\phi}_L \\ \ddot{\theta}_L \\ \ddot{\phi}_R \\ \ddot{\theta}_R \end{bmatrix}. \tag{7}$$

Here, $\phi_{L/R}$ and $\theta_{L/R}$ denote the foot orientation and ankle flexion angles for the left and right legs, respectively.

The matrix $M(q)$ is block-diagonal with inertia submatrices $M_L$ and $M_R$ corresponding to the two pendulums:

$$M(q) = \begin{bmatrix} M_L(\phi_L, \theta_L) & 0 \\ 0 & M_R(\phi_R, \theta_R) \end{bmatrix}. \tag{8}$$

The control torques applied at the ankles are expressed as

$$Q_\tau = \begin{bmatrix} 0 & \tau_L & 0 & \tau_R \end{bmatrix}^\top, \tag{9}$$

while additional generalized forces include:

- $Q_{\text{contact}}$: reaction forces arising from foot–ground interaction, mapped into joint space,
- $Q_{\text{limit}}$: restoring torques that prevent joint excursions beyond anatomical or mechanical bounds,
- $Q_{\text{hip}}$: coupling torques transmitted from pelvis translation and rotation into the two limbs.

This reduced-order model does not capture all complexities of human biomechanics but provides a tractable platform to investigate the combined effects of trajectory generation and passivity control at the ankle joints. By focusing assistance at the distal joints, we highlight how ankle-level actuation influences global stability and center-of-mass dynamics—two critical factors in safe rehabilitation robotics.

In order to simulate the biped model and evaluate the proposed control scheme, we must explicitly compute the angular accelerations $\ddot{q}$, from which angular velocities $\dot{q}$ and configurations $q$ are obtained by numerical integration. The state evolution is governed by

$$\ddot{q} = M(q)^{-1}\Big(Q_\tau + Q_{\text{contact}} + Q_{\text{limit}} + Q_{\text{hip}} - C(q,\dot{q})\dot{q} - G(q)\Big), \tag{10}$$

where the right-hand side combines commanded ankle torques, ground–foot interaction, passive restoring torques, and hip coupling, offset by centrifugal and gravitational effects. This representation highlights the role of ankle actuation within the broader closed-chain dynamics.

**Pelvis dynamics.** Since both legs are coupled through the pelvis, its translational and rotational dynamics must also be considered. The equations of motion for the pelvis are given by:

$$m_{\text{body}}\,\ddot{C}_0 = F_{\text{pelvis}}, \tag{11}$$

$$I_p\,\ddot{\psi} = \underbrace{r_H \times F_{\text{pelvis},L}}_{\text{moment from left leg}} + \underbrace{(-r_H) \times F_{\text{pelvis},R}}_{\text{moment from right leg}} - d_\psi\,\dot{\psi}, \tag{12}$$

where $\ddot{C}_0 = \begin{bmatrix} \ddot{x}_C \\ \ddot{y}_C \end{bmatrix}$ denotes the acceleration of the pelvis center of mass, and $F_{\text{pelvis},L}$ and $F_{\text{pelvis},R}$ are the hip joint reaction forces exerted by the left and right legs. The vector

$$r_H = \tfrac{L_{\text{pelvis}}}{2} \begin{bmatrix} \cos\psi \\ \sin\psi \end{bmatrix}$$

represents the offset from the pelvis center to the left hip (with $-r_H$ to the right hip). Here $I_p$ is the pelvis rotational inertia and $d_\psi$ is a viscous damping term modeling soft-tissue and joint friction around the pelvis.

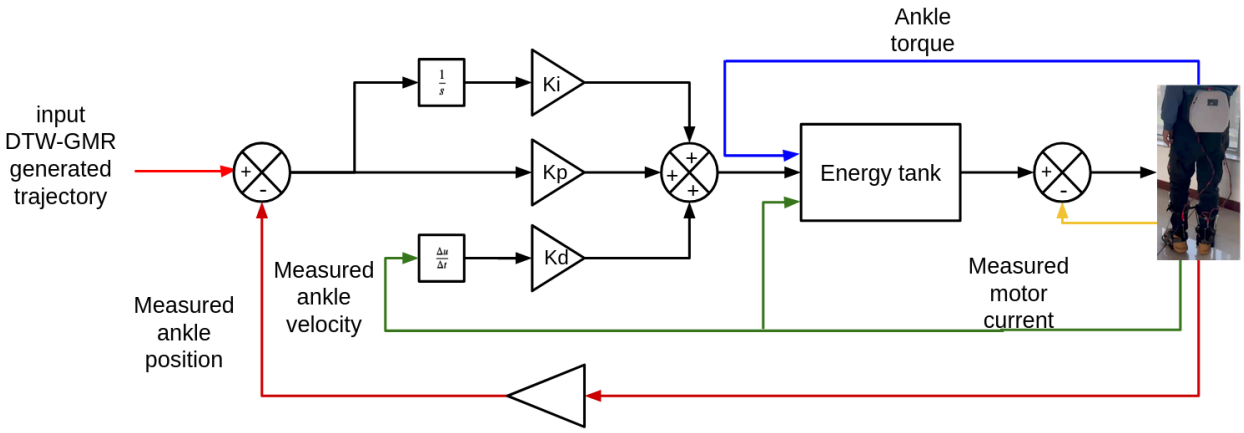


Fig. 5: Block diagram of the ankle exoskeleton control loop with an energy-tank passivity layer. A DTW–GMR reference is tracked by a PID; the energy tank gates the commanded torque to enforce passivity, while encoder and current sensing provide feedback to close the loop

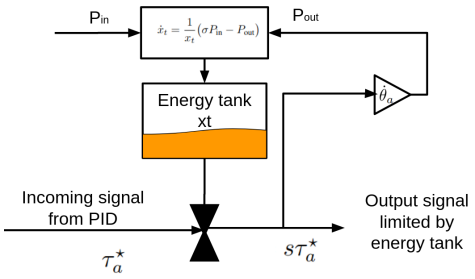


Fig. 6: Schematic representation of the energy tank module. The PID torque request $\tau_a^\star$ is modulated according to the available stored energy $x_t$, ensuring that the output command $s\tau_a^\star$ respects passivity.

## IV. Energy-Tank PID Controller

The control architecture of the ankle exoskeleton is summarized in Fig. 5. Reference trajectories are provided by the DTW–GMR module and tracked by a joint-space PID. To guarantee safe human–robot interaction, the PID output is regulated by an *energy-tank passivity layer*, which adaptively scales the commanded torque according to the available stored energy. Feedback signals include ankle position and velocity from encoders as well as motor current measurements, closing the control loop in hardware-compatible form.

**Principle of the energy tank.** The concept is illustrated in Fig. 6. The PID request $\tau_a^\star$ is filtered through a virtual energy tank, whose storage state $x_t$ defines the energy level

$$T = \tfrac{1}{2}x_t^2, \qquad T \in [T_{\min}, T_{\max}].$$

The tank dynamics are governed by

$$\dot{x}_t = \frac{1}{x_t}\big(\sigma P_{\text{in}} - P_{\text{out}}\big), \tag{13}$$

with the power flows

$$P_{\text{in}} = \max(0, -\tau_a \dot{\theta}_a), \qquad P_{\text{out}} = s\,\big|\tau_a^\star \dot{\theta}_a\big|.$$

Here $\tau_a^\star$ is the torque requested by the PID, while $\tau_a = s\tau_a^\star$ is the final commanded torque. The scaling factor $s \in [0,1]$ modulates assistance: when sufficient energy is stored ($T > T_{\min}$), $s \approx 1$ and the commanded torque tracks the PID output; as the tank depletes, $s \to 0$, limiting assistance and preventing unbounded energy injection. The Boolean $\sigma \in \{0,1\}$ disables charging when the tank is full ($T = T_{\max}$), ensuring bounded storage capacity.

**Interpretation.** This mechanism enforces passivity by construction: dissipative interactions with the user or environment replenish the tank ($P_{\text{in}}$), while active assistance draws from it ($P_{\text{out}}$). In effect, the controller operates under a finite energy budget, which prevents destabilizing behavior even in the presence of modeling errors, timing mismatches, or aggressive reference tracking. From a rehabilitation perspective, this property is essential: it guarantees that the exoskeleton cannot inject unbounded mechanical energy into the user, while still providing meaningful torque support when sufficient dissipative power is available. The result is a controller that balances accuracy, safety, and comfort, making it suitable for clinical translation and eventual real-world deployment.

## V. Simulation Results

### A. Tracking Accuracy with and without Energy Tank

To evaluate the effect of the energy-tank layer, we compared ankle-angle tracking errors under two conditions: plain PID control and PID wrapped with the tank. With the tank enabled, the ankle-angle RMSE decreased from $0.03575$ rad to $0.01707$ rad, corresponding to an error reduction of approximately $52\%$. This improvement was most pronounced during rapid motion phases such as push-off, where the baseline PID exhibited larger deviations from the reference. Representative trajectories are shown in Fig. 7 and Fig. 8,

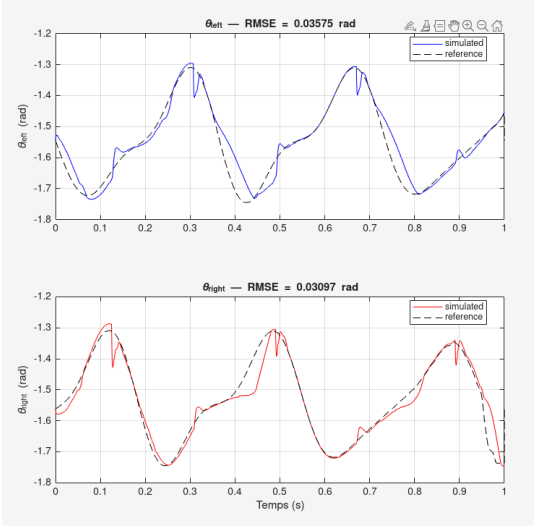


Fig. 7: Left ankle angle tracking without energy tank.

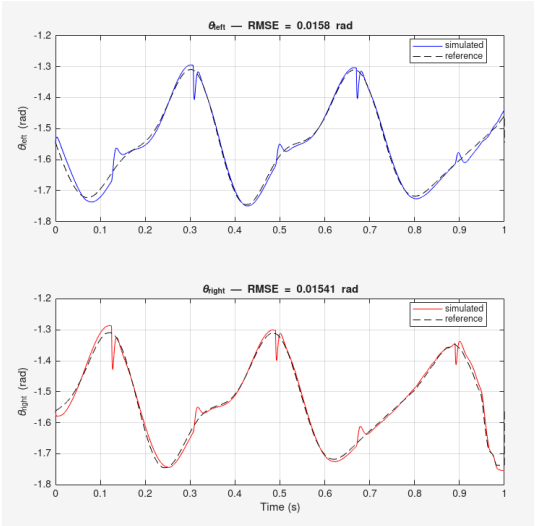


Fig. 8: Left ankle angle tracking with energy tank enabled.

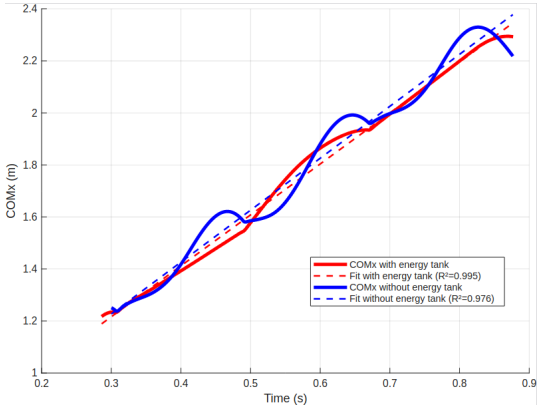


Fig. 9: Effect of the Energy Tank on Center-of-Mass Trajectory Smoothness

which illustrate how the tank-augmented controller produces smoother, more accurate tracking and thereby yields movements that are better suited for rehabilitation.

### B. Center-of-Mass Smoothness and Comfort

Beyond joint-level accuracy, the influence of the passivity constraint on whole-body motion was assessed by examining horizontal center-of-mass ($\mathrm{CoM}_x$) trajectories. Figure 9 compares raw trajectories with polynomial trend fits, where the coefficient of determination quantifies smoothness. With the energy tank enabled, CoM motion exhibited reduced oscillations and a higher fit quality ($R^2 = 0.995$ versus $0.976$ without the tank). This result indicates that the energy tank acts not only as a formal passivity safeguard but also as an adaptive damper, producing more regular whole-body motion that can improve comfort and stability for the user.

## VI. Experimental Results

### A. Experimental Protocol

To evaluate whether the energy-tank controller reduces the mechanical stress experienced by the user, preliminary experiments were conducted with a healthy adult participant (65 kg, 1.70 m). The ankle exoskeleton was worn during level walking while the interaction forces and ankle joint angles were recorded.

The participant was first given time to become familiar with the device and its assistance behavior. Data were then collected over a sequence of ten walking steps. The ankle angle was measured throughout the experiment and compared with the reference trajectories generated by the proposed learning framework.

Three experimental conditions were evaluated:

- tracking of a reference trajectory generated from the GMR model without energy-tank control (PID only),
- tracking of the same GMR-generated trajectory with the energy-tank controller enabled,
- tracking of a contralateral trajectory generated using the symmetry-based reconstruction method.

These experiments aim to assess both the tracking performance of the controller and the influence of the energy-tank mechanism on interaction forces.

### B. Trajectory Following

Figure 10 illustrates the ankle-angle tracking performance for two reference trajectories. Figure 10a corresponds to a trajectory generated using Gaussian Mixture Regression (GMR) trained on recorded gait cycles, whereas Fig. 10b corresponds to a contralateral trajectory reconstructed using the symmetry-based method derived from the same GMR model.

The tracking error for the GMR-trained trajectory resulted in an RMSE of 0.05364 rad, while the symmetry-generated trajectory yielded an RMSE of 0.05852 rad. The largest discrepancies between the measured and reference ankle angles occur during the foot-flat phase of the gait cycle. During this phase, the ankle performs dorsiflexion while the exoskeleton relies on a preloaded spring mechanism

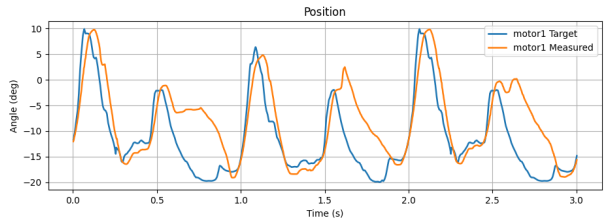


(a) GMR-trained trajectory

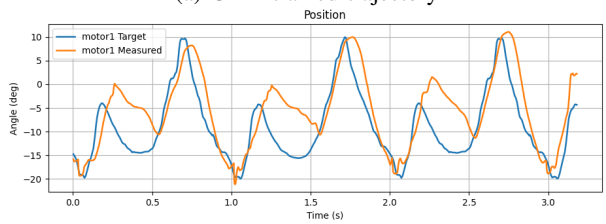


(b) Symmetry-generated trajectory

Fig. 10: Comparison of reference trajectories used for ankle tracking.

to generate the corresponding torque. Because this spring produces a nearly constant restoring force that is difficult to modulate precisely, the interaction between the spring force and the user's voluntary muscle torque can lead to deviations from the reference trajectory.

Despite this effect, the RMSE values obtained with the two trajectory-generation methods remain comparable. This result suggests that the symmetry-based trajectory reconstruction provides a viable alternative when contralateral sensing is unavailable, supporting the feasibility of unilateral sensing for rehabilitation applications.

### C. Energy Tank Control

Figure 11 compares the ankle-angle tracking performance obtained with a conventional PID controller and with the proposed energy-tank-based controller. In each case, the measured ankle angle is shown together with the reference trajectory, along with the corresponding cable force generated by the actuator.

The PID controller achieves a lower tracking error, with an RMSE of 0.05236 rad, compared with 0.06862 rad for the energy-tank controller. However, the energy-tank mechanism significantly reduces the peak interaction force applied by the actuator. The maximum cable force decreases from approximately 120 N under PID control to 80 N when the energy tank is enabled.

This reduction in peak force illustrates the trade-off introduced by the passivity constraint. While the energy-tank controller slightly degrades tracking accuracy, it effectively limits the mechanical effort transmitted to the user. From a rehabilitation perspective, this behavior is desirable, as it reduces excessive forces on the joint and can improve user comfort and safety during assisted walking.

## VII. Discussion

Taken together, the results highlight three complementary observations regarding trajectory generation and passivity-based control for ankle exoskeleton assistance.

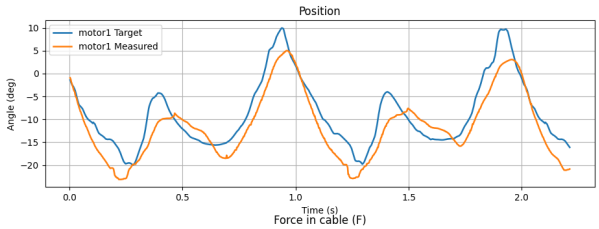


(a) PID controller

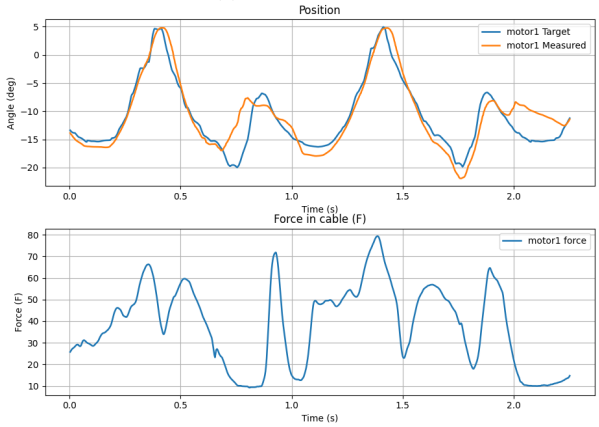


(b) Energy-tank controller

Fig. 11: Comparison between standard PID control and energy-tank-based control.

First, the DTW–GMR reference learning pipeline enables phase-consistent ankle trajectories that remain stable across gait cycles. The alignment provided by DTW prevents temporal smearing of key gait events, while the probabilistic synthesis of GMR produces smooth templates that preserve the variability structure of the recorded data. As observed both in simulation and in hardware experiments, these references can be tracked with relatively small angular errors, demonstrating their suitability for exoskeleton control.

Second, the symmetry-based trajectory reconstruction provides a practical strategy when only unilateral sensing is available. The experimental results show that trajectories generated through symmetry yield tracking errors comparable to those obtained with directly learned GMR references. Although small discrepancies appear during the foot-flat phase, likely due to the interaction between the user's voluntary dorsiflexion torque and the exoskeleton's spring mechanism, the overall RMSE values remain similar. This suggests that symmetry-based reconstruction can serve as a viable alternative for generating contralateral references in rehabilitation contexts where bilateral sensing is not feasible.

Third, the experimental comparison between conventional

PID control and the energy-tank controller highlights the fundamental trade-off introduced by passivity enforcement. While the standard PID controller achieves slightly better trajectory tracking accuracy, the energy-tank controller significantly reduces the peak interaction forces applied by the actuator (approximately 80 N compared with 120 N). This behavior is consistent with the role of the energy tank as a virtual energy reservoir that limits the mechanical energy injected into the human–robot system. From a rehabilitation perspective, this reduction in peak forces may improve user comfort and safety, even at the cost of a modest increase in tracking error.

Several limitations remain in the present study. The experimental evaluation was conducted with a single healthy participant and a limited number of walking steps, which does not fully capture the variability encountered in real rehabilitation scenarios. Furthermore, the mechanical design of the exoskeleton relies on a spring-based actuation mechanism for dorsiflexion assistance, which introduces forces that are difficult to modulate precisely and may contribute to the tracking deviations observed during the foot-flat phase.

## VIII. Conclusion

This paper presented a unified framework for ankle exoskeleton assistance that combines phase-consistent trajectory learning with passivity-based control. Reference ankle trajectories were generated from wearable IMU data using Dynamic Time Warping (DTW) alignment and Gaussian Mixture Regression (GMR), producing smooth subject-specific templates robust to variations in gait timing. When only unilateral sensing is available, contralateral trajectories can be reconstructed through symmetry-based mappings, enabling bilateral assistance from a single instrumented limb.

On the control side, a joint-space PID controller was augmented with an energy-tank passivity layer that regulates the mechanical energy exchanged between the exoskeleton and the user. Simulation results showed that this approach produces smoother center-of-mass motion.

Preliminary experiments with a wearable ankle exoskeleton further illustrate the practical impact of the approach. Although the conventional PID controller achieved slightly lower tracking error, the energy-tank controller reduced the peak interaction force from approximately 120 N to 80 N. This result highlights the safety–performance trade-off of passivity-based control: limiting injected energy can slightly reduce tracking accuracy but improves interaction safety and user comfort.

Overall, coupling phase-consistent trajectory learning with energy-bounded control provides a promising strategy for safe and adaptive ankle exoskeleton assistance. Future work will extend the experimental evaluation to larger participant groups and impaired populations, and investigate online trajectory generation from streaming IMU data together with adaptive energy-tank strategies.

## References


[1] V. L. Feigin, et al., "Global, regional, and national burden of stroke and its risk factors, 1990–2019," *The Lancet Neurology*, 20(10):795–820, 2021.

[2] Srivastava et al., "Assist-as-Needed Robot-Aided Gait Training Improves Walking Function in Individuals Following Stroke," IEEE Transactions on Neural Systems and Rehabilitation Engineering, vol. 23, no. 6, pp. 956–963.

[3] Nam, Ki Yeun, et al. "Robot-assisted gait training (Lokomat) improves walking function and activity in people with spinal cord injury: a systematic review." Journal of neuroengineering and rehabilitation 14.1 (2017): 24.

[4] S. H. Collins, et al., "Reducing the energy cost of human walking using an unpowered exoskeleton," *Nature*, 522:212–215, 2015;

[5] F. Petitjean, A. Ketterlin, and P. Gancarski, "A global averaging method for dynamic time warping, with applications to clustering," *Pattern Recognition*, 44(3):678–693, 2011; and F. Petitjean and P. Gançarski, "DTW Barycenter Averaging," *Pattern Recognition*, 47(12):3811–3826, 2014.

[6] P. Senin, "Dynamic Time Warping Algorithm Review," Univ. Hawaii Technical Report, 2008.

[7] S. Calinon, "A tutorial on task-parameterized movement learning and retrieval," *Intelligent Service Robotics*, 9(1):1–29, 2016.

[8] Patterson, K. K., Gage, W. H., Brooks, D., Black, S. E., and McIlroy, W. E. (2010). Evaluation of gait symmetry after stroke: a comparison of current methods and recommendations for standardization. Gait and posture, 31(2), 241-246.

[9] F. Ferraguti, C. Secchi, and C. Fantuzzi, "A tank-based approach to impedance control with variable stiffness," in *Proc. IEEE ICRA*, pp. 4948–4953, 2013.

[10] A. Dietrich, et al., "Passive hierarchical impedance control via energy tanks," *IEEE Robotics and Automation Letters*, 3(4):2878–2885, 2018.

[11] DING, Zhangchi, BAGHBAHARI, Masoud, et BEHAL, Aman. A passivity-based framework for safe physical human–robot interaction. Robotics, 2023, vol. 12, no 4, p. 116.

[12] D. Roetenberg, H. Luinge, and P. Slycke, "Xsens MVN: Full 6DOF human motion tracking using miniature inertial sensors," Xsens Technologies, Technical Report, 2009.

[13] H. Luinge and P. Veltink, "Measuring orientation of human body segments using miniature gyroscopes and accelerometers," *Med. & Biol. Eng. & Comput.*, 43(2):273–282, 2005.

[14] M. Müller, "Dynamic Time Warping," in *Information Retrieval for Music and Motion*, Springer, pp. 69–84, 2007.

[15] S. Calinon, F. Guenter, and A. Billard, "On learning, representing, and generalizing a task in a humanoid robot," *IEEE Trans. SMC—Part B*, 37(2):286–298, 2007.

[16] J. M. Finley and A. J. Bastian, "Associating locomotor performance with locomotor learning in people with stroke," *J. Neurol. Phys. Ther.*, 41(4):241–250, 2017; and J. M. Finley, et al., "Learning to be economical: The energy cost of step length asymmetry," *J. Neurophysiol.*, 118(3):1696–1708, 2017.

[17] A. Mannini and A. M. Sabatini, "Gait phase detection and discrimination between walking–jogging activities using accelerometers," *Sensors*, 12(6): 6532–6545, 2012; see also A. Mannini, et al., "A hidden Markov model-based technique for gait segmentation using a foot-mounted gyroscope," *Med. & Biol. Eng. & Comput.*, 48(2):153–161, 2010.

[18] M. Błażkiewicz, "Gait Symmetry Analysis Based on Dynamic Time Warping," *Symmetry*, vol. 13, no. 5, p. 836, 2021.

[19] J. R. Koller, C. D. Remy, and D. P. Ferris, "Biomechanics and energetics of walking in powered ankle exoskeletons using myoelectric control versus mechanically intrinsic control," *Journal of NeuroEngineering and Rehabilitation*, vol. 15, no. 1, p. 42, 2018.

[20] B. A. Shafer, S. A. Philius, R. W. Nuckols, J. McCall, A. J. Young, and G. S. Sawicki, "Neuromechanics and energetics of walking with an ankle exoskeleton using neuromuscular-model based control: a parameter study," *Frontiers in Bioengineering and Biotechnology*, vol. 9, Art. no. 615358, 2021.